

SDSSp J104433.04–012502.2 at $z = 5.74$ is Gravitationally Magnified by an Intervening Galaxy^{*}

Yasuhiro SHIOYA¹, Yoshiaki TANIGUCHI¹, Takashi MURAYAMA¹, Masaru AJIKI¹,
Tohru NAGAO¹, Shinobu S. FUJITA¹, Yuko KAKAZU², Yutaka KOMIYAMA³,
Sadanori OKAMURA^{4,5}, Shinki OYABU⁶, Kimiaki KAWARA⁶, Youichi OHYAMA³,
Koji S. KAWABATA⁷, Hiroyasu ANDO³, Tetsuo NISHIMURA³, Masahiko HAYASHI³,
Ryusuke OGASAWARA³, & Shin-ichi ICHIKAWA⁷

¹*Astronomical Institute, Graduate School of Science, Tohoku University, Aramaki, Aoba,
Sendai 980-8578*

shioya@astr.tohoku.ac.jp

²*Institute for Astronomy, University of Hawaii, 2680 Woodlawn Drive, Honolulu, HI 96822, USA*

³*Subaru Telescope, National Astronomical Observatory of Japan, 650 N.A'ohoku Place, Hilo, HI 96720, USA*

⁴*Department of Astronomy, Graduate School of Science, The University of Tokyo, Tokyo 113-0033*

⁵*Research Center for the Early Universe, School of Science, The University of Tokyo, Tokyo 113-0033*

⁶*Institute of Astronomy, Graduate School of Science, The University of Tokyo, 2-21-1 Osawa, Mitaka,
Tokyo 181-0015*

⁷*National Astronomical Observatory, 2-21-1 Osawa, Mitaka, Tokyo 181-8588*

(Received 2002 June 18; accepted 2002 October 6)

Abstract

During the course of our optical deep survey program on $L\alpha$ emitters at $z \approx 5.7$ in the sky area surrounding the quasar SDSSp J104433.04–012502.2 at $z = 5.74$, we found that a faint galaxy with $m_B(\text{AB}) \approx 25$ is located at $1''.9$ southwest of the quasar. Its broad-band color properties from B to z' suggest that the galaxy is located at a redshift of $z \sim 1.5 - 2.5$. This is consistent with no strong emission line in our optical spectroscopy. Since the counter image of the quasar cannot be seen in our deep optical images, the magnification factor seems not to be very high. Our modest estimate is that this quasar is gravitationally magnified by a factor of 2.

Key words: gravitational lensing — galaxies: high-redshift — galaxies: quasars: individual (SDSSp J104433.04–012502.2)

^{*} Based on data collected at Subaru Telescope, which is operated by the National Astronomical Observatory of Japan.

1. Introduction

The Sloan Digital Sky Survey (SDSS: e.g., York et al. 2000) has been finding high-redshift quasars at $z \approx 6$; the most distant known to date is SDSSp J103027.10+052455.0 at $z = 6.28$ (Fan et al. 2000, 2001). One serious problem seems to be that all of these $z \sim 6$ SDSS quasars are exceptionally bright (see table 1). As claimed by Wyithe and Loeb (2002; hereafter WL02), the presence of such very bright quasars at $z \sim 6$ raises the following two problems: (1) If the central engine of these quasars is an accreting supermassive black hole and shines near the Eddington accretion rate, a supermassive black hole with mass exceeding $\sim 3 \times 10^9 M_\odot$ was already formed beyond $z = 6$. This challenges models for early structure formation (Turner 1991; Haiman, Loeb 2001). Also, (2) the absolute luminosities of the $z \sim 6$ quasars are systematically higher than expected from the SDSS survey criteria (Fan et al. 2000, 2001), suggesting that the luminosity function of the $z \sim 6$ quasars is significantly biased to higher luminosities. These two problems urge WL02 to propose that the SDSS $z \sim 6$ quasars may be magnified by intervening gravitational lenses.

During the course of our optical deep survey program on $L\alpha$ emitters at $z \approx 5.7$ in the field surrounding the quasar SDSSp J104433.04–012502.2 at $z = 5.74$, we found that a faint galaxy with $m_B(\text{AB}) \approx 25$ is located at $1''.9$ southwest of this quasar. In this paper, we report on the possibility that SDSSp J104433.04–012502.2 is gravitationally magnified by a faint galaxy with optical photometric and spectroscopic data obtained by our observations. Throughout this paper, we adopt a flat universe with $\Omega_m = 0.3$, $\Omega_\Lambda = 0.7$, and $h = 0.7$, where $h = H_0/(100 \text{ km s}^{-1} \text{ Mpc}^{-1})$.

2. Optical Deep Imaging

Deep optical imaging observations were made with the Suprime-Cam (Miyazaki et al. 1998) on the 8.2 m Subaru telescope (Kaifu 1998) at Mauna Kea Observatories. The Suprime-Cam consists of ten $2k \times 4k$ CCD chips and provides a very wide field of view: $34' \times 27'$ with a $0''.2/\text{pixel}$ resolution. Therefore, the combination between the Suprime-Cam and the Subaru telescope enables us to carry out wide and deep narrow-band imaging surveys for high- z emission-line objects. Using this facility, we made a very deep optical imaging survey for faint $L\alpha$ emitters in the field surrounding the SDSSp J104433.04–012502.2 at a redshift of 5.74 (Fan et al. 2000; Djorgovski et al. 2001; Goodrich et al. 2001). In this survey, we used a narrow-passband filter, NB816, centered at 8160 \AA with a passband of $\Delta\lambda(\text{FWHM}) = 120 \text{ \AA}$; the central wavelength corresponds to a redshift of 5.72 for $L\alpha$ emission. We also used broad-passband filters: B , R_C , I_C , and z' . A summary of the imaging observations is given in table 2. All of the observations were made under photometric conditions, and the seeing size was between $0''.7$ and $1''.3$ during the run.

In this paper, we analyze only two CCD chips in which the quasar SDSSp

J104433.04–012502.2 is included (see also Ajiki et al. 2002). The field size is $11'.67$ by $11'.67$. The individual CCD data were reduced and combined using IRAF and mosaic-CCD data-reduction software developed by Yagi et al. (2002). The photometric and spectrophotometric standard stars used in the flux calibration were SA101 for the B , R_C , and I_C data, and GD 50, GD 108 (Oke 1990), and PG 1034+001 (Massey et al. 1996) for the NB816 data. The z' data were calibrated using the magnitude of SDSSp J104433.04–012502.2 (Fan et al. 2000). Thumb-nail optical images of the quasar field are shown in figure 1. A faint galaxy is seen at $1''.9$ southwest from the quasar. This galaxy is seen even in the B -band image, giving a rough constraint such that its redshift is $z < 2.6$, since the wavelength of redshifted $L\alpha$ absorptions by intergalactic neutral hydrogen is considered to be shorter than about 4400 \AA .

3. Optical Spectroscopy

In order to estimate a spectroscopic redshift, we carried out optical spectroscopy using the Subaru Faint Object Camera And Spectrograph (FOCAS; Kashikawa et al. 2000) on 2002 March 13 (UT). We used $300 \text{ lines mm}^{-1}$ grating blazed at 7500 \AA (300R) together with an order cut filter SY47, giving a spectral resolution of $R \simeq 1000$ with a $0''.8$ -wide slit. This setting gave a wavelength coverage between 4700 \AA and 9400 \AA . The integration time was 1800 s. The spectrum is shown in figure 2. This spectrum shows that this galaxy has blue colors, and that there is no prominent emission line. If this galaxy is a strong emission-line galaxy, like a starburst galaxy, it is inferred either that its redshifted wavelength of $L\alpha$ emission line would be shorter than 4700 \AA , or that its redshifted wavelength of $[\text{O II}]\lambda 3727$ emission line would be longer than 9400 \AA . From these constraints, one may estimate that the redshift of this galaxy lies in a range between $z \approx 1.5$ and $z \approx 2.9$.

4. Results and Discussion

The faint galaxy which we have found (hereafter, the lens galaxy) is located at $1''.9$ southwest from the quasar. In order to estimate how the quasar is gravitationally magnified, we need information about both the redshift and the stellar velocity dispersion of this lens galaxy. However, no direct information on these two quantities was obtained in our observations. Therefore, in this paper, first, we estimate its photometric redshift based on our optical broadband photometric data (subsection 4.1). Second, we also estimate its stellar velocity dispersion using the Tully—Fisher relation (subsection 4.2). Then, we estimate the magnification factor based on the singular isothermal sphere model for gravitational lensing (subsection 4.3).

4.1. Photometric Redshift of the Lens Galaxy

Using optical B , R_C , I_C , NB816, and z' data, we estimated a probable photometric redshift of the lens galaxy. Its optical magnitudes obtained in our observations were $B = 25.1 \pm 0.06$, $R_C = 24.5 \pm 0.04$, $I_C = 24.3 \pm 0.06$, NB816 = 24.2 ± 0.04 , and $z' = 23.9 \pm 0.09$;

the quoted errors are 1σ sky noises. It is noted again that because the lens galaxy is not a B -dropout, we had a constraint of $z < 2.62$.

A photometric redshift of a galaxy was evaluated from the global shape of the spectral energy distribution (SED) of a galaxy, as a redshift with the maximum likelihood,

$$L(z, t) = \prod_{i=1}^5 \exp \left\{ -\frac{1}{2} \left[\frac{f_i - AF_i(z, t)}{\sigma_i} \right]^2 \right\}, \quad (1)$$

where f_i , $F_i(z, t)$, and σ_i are the observed flux, the template flux, and the error of the i -th band, respectively, and A is defined as

$$A = \frac{\sum F_i f_i / \sigma_i^2}{\sum F_i^2 / \sigma_i^2}. \quad (2)$$

The SED of a galaxy that we observed was mainly determined by the following four factors: (1) the radiation from stars in the galaxy, (2) the extinction by dust in the galaxy, itself, (3) the redshift of the galaxy, and (4) the absorption by the intergalactic neutral hydrogen between the galaxy and us. We treated the above factors in the following way.

We used the population synthesis model GISSEL96, which is a revised version of Bruzual and Charlot (1993) (see also Leitherer et al. 1996), to calculate an SED from stellar components. The SED of the galaxy was determined by its star-formation history. The SEDs of local galaxies were well reproduced by models whose star-formation rate declines exponentially (τ model); i.e., $SFR(t) \propto \exp(-t/\tau)$, where t is the age of the galaxy and τ is the time scale of star formation. Different combinations of t and τ generate a similar shape of SED. In this work, we therefore used $\tau = 1$ Gyr models with the Salpeter's initial mass function (the power index of $x = 1.35$ and the stellar mass range of $0.01 \leq m/M_\odot \leq 125$) to derive various SED types. We adopted the solar metallicity, $Z = 0.02$. For these models, we calculated SEDs with ages of $t = 0.1, 0.5, 1, 2, 3, 4$, and 8 Gyr, and called them SED1, SED2, SED3, SED4, SED5, SED6, and SED7, respectively; note that the SED templates derived by Coleman et al. (1980), elliptical galaxies (the bulges of M 31 and M 81), Sbc, Scd, and Irr correspond to those of SED7 ($t = 8$ Gyr), SED6 ($t = 4$ Gyr), SED5 ($t = 3$ Gyr), and SED4 ($t = 2$ Gyr), respectively. We adopted the dust extinction curve for starburst galaxies determined by Calzetti et al. (2000) with visual extinctions of $A_V = 0, 0.2, 0.4, 0.6, 0.8$, and 1.0. As for the absorption by intergalactic neutral hydrogen, we used the average optical depth derived by Madau et al. (1996). However, Scott, Bechtold, and Dobrzycki (2000) showed that the observed continuum depression between 1050 $(1+z)$ Å and 1170 $(1+z)$ Å due to the $L\alpha$ clouds (D_A) for quasars with $z \lesssim 3$ is lower than that expected from extrapolation using the cosmic transmission derived by Madau et al. (1996). Further, they also showed that there is a scatter in D_A from quasar to quasar. Therefore, we also investigated the following two cases: 1) $0.5 \times$ the Madau et al.'s average optical depth, and 2) $2 \times$ the Madau et al.'s average optical depth. We then estimated the probable photometric redshift of the lens galaxy. In this procedure, we adopted an allowed redshift of between $z = 0$ and $z = 6$ with a redshift bin of $\Delta z = 0.02$.

Our results are shown in figure 3. In this figure, we show the distributions of the likelihood for the seven SEDs. Our best estimate of the photometric redshift of the lens galaxy is $z_{\text{phot}} \approx 2.1$. Since the likelihood, $L(z, T)$, exceeds 0.1 for $z \sim 1.5 - 2.5$, it is suggested that the lens galaxy is located at $1.5 < z < 2.5$. This range is consistent with the information from our optical spectroscopy (section 3). SED1 appears to be inappropriate for the SED of the lens galaxy. It is found that SED7 also has a maximum likelihood larger than 0.1 around $z \sim 3$. However, since the age of the galaxy at $z \sim 3$ is considered to be younger than 2 Gyr, we also threw out SED7. The luminosity of the galaxy was evaluated to be the normalization factor, A , times the luminosity of the model. The range of the evaluated absolute B -band magnitude for SED2 through SED6 was between $z = 1.5$ and 2.5 is $-20.4 > M_B > -23.1$.

4.2. *Stellar Velocity Dispersion of the Lens Galaxy*

Although it is necessary for the estimate of the magnification factor by gravitational lensing to know the stellar velocity dispersion (σ_v) of the lens galaxy, there is no direct measurement. Given the redshift of a lens galaxy, we could estimate its absolute magnitude and then estimate a probable value of the stellar velocity dispersion. Since it is considered that the lens galaxy is located at $1.5 < z < 2.5$, we could estimate the stellar velocity dispersion as a function of both the redshift and SED based on the Tully—Fisher relation established for a sample of galaxies in the local universe.

Here, we used the Tully—Fisher relation derived by Sakai et al. (2000),

$$M_B = -8.07(\log W_{20} - 2.5) - 19.88, \quad (3)$$

where M_B is the absolute B magnitude and W_{20} is the full width at 20% of the maximum velocity. Assuming that $\sigma_v = V_{\text{rot}}/\sqrt{2} = W_{20}/2\sqrt{2}$ where V_{rot} is the rotation velocity, we estimated σ_v as a function of z and SED. We evaluated M_B using the method given in subsection 4.1. The results are shown in figure 4. Since the cases of SED1 and SED7 are rejected in subsection 4.1, the velocity dispersion is estimated to be in a range between 140 km s^{-1} and 280 km s^{-1} for a redshift range of $1.5 < z < 2.5$.

4.3. *Magnification Factor by the Gravitational Lensing*

We are now ready to estimate the magnification factor by gravitational lensing. We adopt the singular isothermal sphere (SIS) model for simplicity (e.g., Binney, Merrifield 1998). In this model, the magnification factor for the brighter source can be expressed as

$$M_+ = \frac{\theta}{\theta - \theta_E}, \quad (4)$$

where θ is the angle between the lens galaxy and the source (i.e., SDSSp J104433.04–012502.2 in this case), and the θ_E is the Einstein angle, defined as

$$\theta_E = 4\pi \left(\frac{\sigma_v}{c} \right)^2 \frac{D_{\text{LS}}}{D_{\text{OS}}}, \quad (5)$$

where D_{LS} is the angular diameter distance between the lens galaxy and the source and D_{OS} is that between the observer and the source. In figure 5, we show the magnification factor as a function of z for eight cases of $\sigma_v = 140, 160, 180, 200, 220, 240, 260$, and 280 km s^{-1} . In this figure, we also show the magnification factor for the counter image [$M_- = \theta/(\theta_E - \theta)$], which can be seen at $\theta = \theta_E - \beta$, where β is the angle between the lens galaxy and the intrinsic source. If the lens galaxy is located at $z \sim 2$ and has $\sigma_v \sim 280 \text{ km s}^{-1}$, θ_E becomes $1''.9$ and we thus obtain $M_+ = \text{infinity}$. However, if this is the case, since $\beta \sim 0$ and $M_- \sim M_+$, we would observe the counter image with nearly the same brightness as that of the lensed image. Further, if $M_+ > 10$, M_- is also as large as M_+ . As we shown in figure 1 that there is no apparent object, except the quasar ($z' = 19.2 \text{ mag}$) and the lens galaxy ($z' = 23.9$). Since there is no apparent counter image, the magnification factor must be much less than 10. If $\sigma_v \lesssim 200 \text{ km s}^{-1}$, the condition of $M_- \ll M_+$ is achieved at $z \sim 2$. In this case, we obtain $M_+ \sim 2$.

4.4. Concluding Remarks

We have found a candidate of a lensing galaxy at $1''.9$ southwest of the SDSS high- z quasar, SDSSp J104433.04–012502.2. From our observational data, we find that the lens galaxy is located at $1.5 < z < 2.5$; the most probable photometric redshift is $z_{\text{phot}} \approx 2.1$. Adopting the SIS model for gravitational lensing, we estimate the magnification factor to be $M_+ \sim 2$ if the lens galaxy is located at $z \sim 2$ and has a stellar velocity dispersion of $\sigma_v \sim 200 \text{ km s}^{-1}$.

WL02 suggested that the SDSS $z \sim 6$ quasars are systematically brighter than expected. Namely, they investigated the probability that a quasar with a rest-frame 1450 \AA magnitude, $M_{1450}(\text{AB})$, and a redshift of z was selected into the survey using the survey selection function given in Fan et al. (2001). They found that the cumulative probability of $M_{1450}(\text{AB})$ for the $z \sim 6$ quasars is different from the expected one at the 95% significance level. However, they also suggested that this inconsistency is removed if the flux of one or more of the $z \sim 6$ quasars is overestimated by a factor of 2. Therefore, our finding presented in this paper may remove the inconsistency raised by WL02.

It is known that the lensing optical depth increases with increasing the redshift, and thus objects at higher redshift are more affected by gravitational lensing from a statistical point of view (e.g., Turner 1991; Barkana, Loeb 2000; WL02). As proposed by WL02, it will be very important to carefully search for lensing galaxies towards all high- z quasars by deep and high-resolution imaging.

We would like to thank the Subaru Telescope staff for their invaluable help. We also thank Dr. Hayashino for his invaluable help. This work was financially supported in part by the Ministry of Education, Culture, Sports, Science, and Technology (Nos. 10044052 and 10304013).

References

- Ajiki, M., Taniguchi, Y., Murayama, T., Nagao, T., Veilleux, S., Shioya, Y., Fujita, S. S., Kakazu, Y. 2002, *ApJ*, 576, L25
- Barkana, R., & Loeb, A. 2000, *ApJ*, 531, 613
- Binney, J., & Merrifield, M. 1998, *Galactic Astronomy*, (Princeton, New Jersey, Princeton University Press), Ch. 2.4
- Bruzual, A. G., & Charlot, S. 1993, *ApJ*, 405, 538
- Calzetti, D., Armus, L., Bohlin, R. C., Kinney, A. L., Koornneef, J., & Storchi-Bergmann, T. 2000, *ApJ*, 533, 682
- Coleman, G. D., Wu, C.-C., & Weedman, D. W. 1983, *ApJS*, 43, 393
- Djorgovski, S. G., Castro, S., Stern, D., & Mahabal, A. A. 2001, *ApJ*, 560, L5
- Fan, X., Narayanan, V. K., Lupton, R. H., Strauss, M. A., Knapp, G. R., Becker, R. H., White, R. L., Pentericci, L., et al. 2001, *AJ*, 122, 2833
- Fan, X., White, R. L., Davis, M., Becker, R. H., Strauss, M. A., Haiman, Z., Schneider, D. P., Gregg, M. D., et al. 2000, *AJ*, 120, 1167
- Goodrich, R. W., Campbell, R., Chaffee, F. H., Hill, G. M., Sprayberry, D., Brandt, W. N., Schneider, D. P., Kaspi, S., et al. 2001, *ApJ*, 561, L23
- Haiman, Z., & Loeb, A. 2001, 503, 505
- Kaifu, N. 1998, *Proc. SPIE*, 3352, 14
- Kashikawa, N., Inata, M., Iye, M., Kawabata, K., Okita, K., Kosugi, G., Ohyama, Y., Sasaki, T. et al. 2000, *Proc. SPIE*, 4008, 104
- Leitherer, C., Alloin, D., Fritze-von Alvensleben, U., Gallagher, J. S., Huchra, J. P., Matteucci, F., O'Connell, R. W., Beckman, J. E., et al. 1996, *PASP*, 108, 966
- Madau, P., Ferguson, H. C., Dickinson, M. E., Giavalisco, M., Steidel, C. C., & Fruchter, A. 1996, *MNRAS*, 283, 1388
- Massey, P., Strobel, K., Barnes, J. V., & Anderson, E. 1988, *ApJ*, 328, 315
- Miyazaki, S., Sekiguchi, M., Imi, K., Okada, N., Nakata, F., & Komiyama, Y. 1998, *Proc. SPIE*, 3355, 363
- Oke, J. B. 1990, *AJ*, 99, 1621
- Sakai, S., Mould, J. R., Hughes, S. M. G., Huchra, J. P., Macri, L. M., Kennicutt, R. C., Jr., Gibson, B. K., Ferrarese, L., et al. 2000, *ApJ*, 529, 698
- Scott, J., Bechtold, J., & Dobrzycki, A. 2000, *ApJS*, 130, 37
- Turner, E. L. 1991, *AJ*, 101, 5
- Vanden Berk, D. E., Richards, G. T., Bauer, A., Strauss, M. A., Schneider, D. P., Heckman, T. M., York, D. G., Hall, P. B., et al. 2001, *AJ*, 122, 549
- Wyithe, J. S. B., & Loeb, A. 2002, *Nature*, 417, 923 (WL02)
- Yagi M., Kashikawa, N., Sekiguchi, M., Doi, M., Yasuda, N., Shimasaku, K., & Okamura, S. 2002, *AJ*, 123, 66
- York, D. G., Adelman, J., Anderson, J. E., Jr., Anderson, S. F., Annis, J., Bahcall, N. A., Bakken, J. A., Barkhauser, R., et al. 2000, *AJ*, 120, 1579

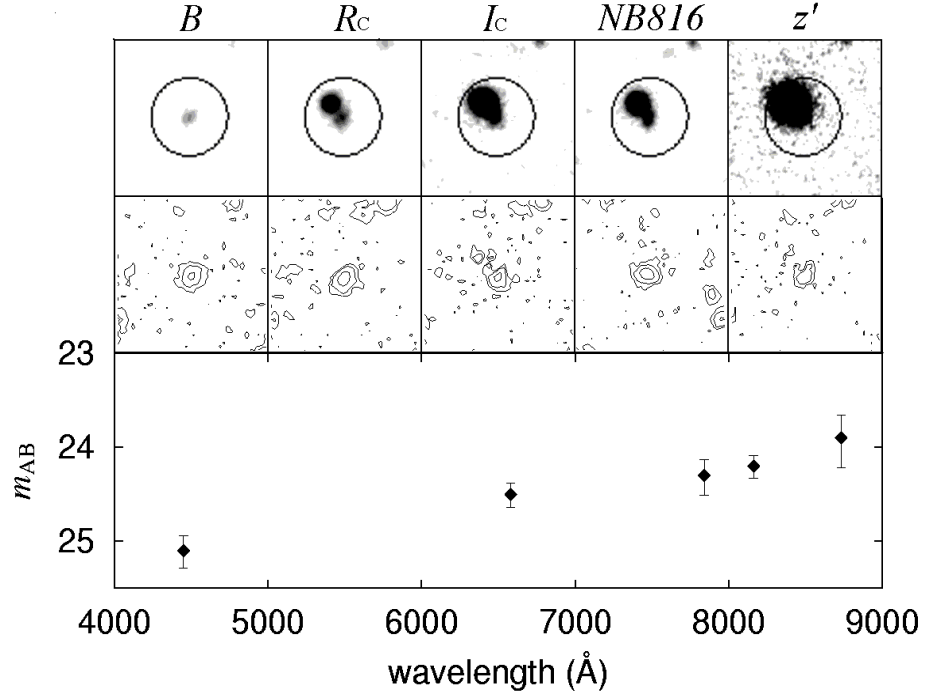


Fig. 1. Thumb-nail images of SDSSp J104433.04-012502.2 and its neighbor galaxy (upper panel). The angular size of the circle in each panel corresponds to 8''. A contour plot of a lens galaxy after the quasar had been subtracted is shown in the middle panel. The lower panel shows the spectral energy distribution of the neighbor galaxy in the magnitude scale.

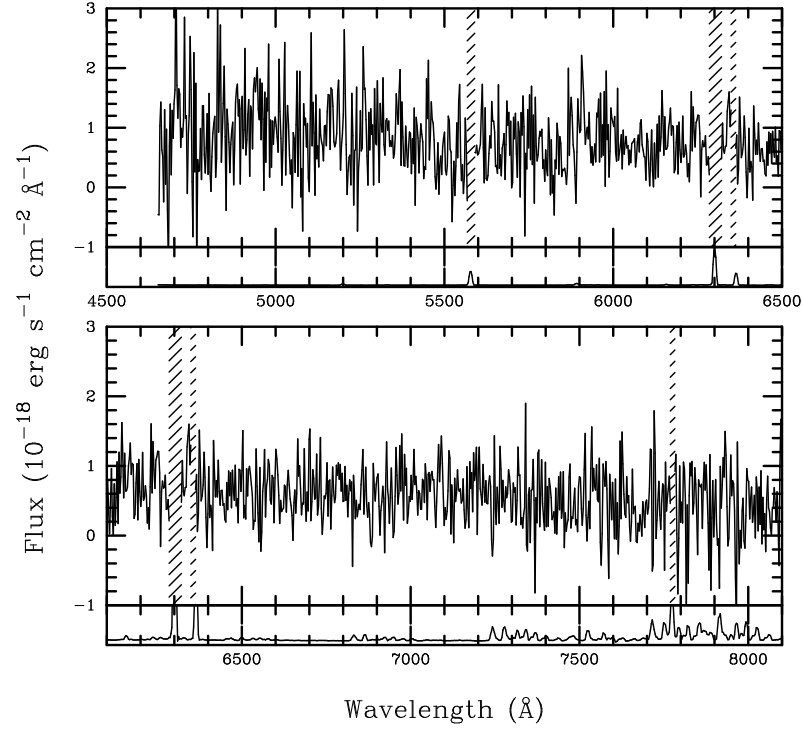


Fig. 2. Optical spectrum of the neighboring galaxy. The hatched regions indicate the positions of the strong night sky lines. The sky spectrum is also shown in the lower part of each panel.

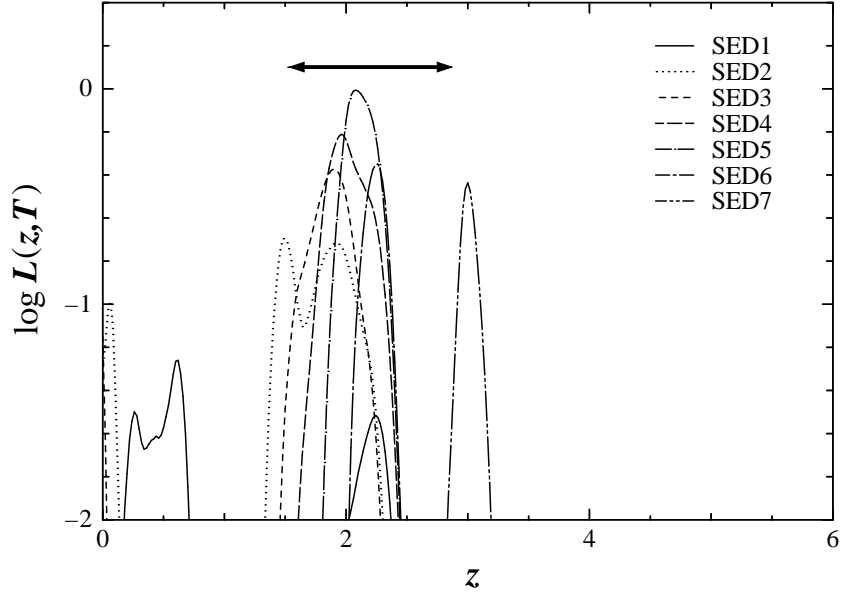


Fig. 3. Distributions of the likelihood for the seven SEDs shown as a function of the redshift. The arrow in the upper part shows the range of the probable redshift of the galaxy estimated by optical spectroscopy.

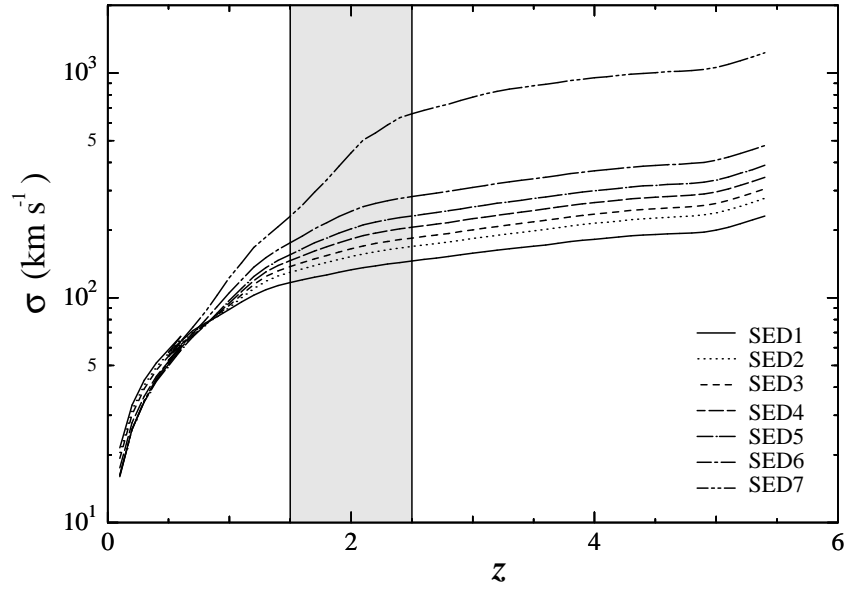


Fig. 4. Distributions of the velocity dispersion of the lens galaxy shown as a function of the redshift for seven SEDs.

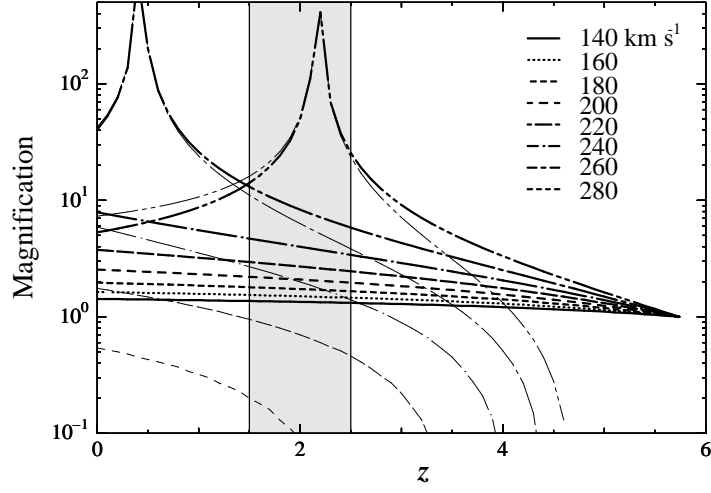


Fig. 5. Distributions of the magnification factor of the source observed at $\theta = 1''.9$ (thick lines) and its counter image (thin lines) shown as a function of the redshift for the eight cases for the stellar velocity dispersion. We assume the magnification of the former one to be M_+ , except for the case that θ is smaller than θ_E .

Table 1. List of $z \sim 6$ SDSS quasars.

Name	Redshift	z'	M_B^*
SDSSp J104433.04−012502.2	5.74 [†]	19.20	−28.09
SDSSp J083643.85+005453.3	5.82	18.74	−28.54
SDSSp J130608.26+035626.3	5.99	19.47	−27.73
SDSSp J103027.10+052455.0	6.28	20.05	−27.23

*The k -correction was made by using the composite quasar spectrum in Vanden Berk et al. (2001).

[†]The discovery redshift was $z = 5.8$ (Fan et al. 2000). Since, however, the subsequent optical spectroscopic observations suggested a bit lower redshift; $z = 5.73$ (Djorgovski et al. 2001) and $z = 5.745$ (Goodrich et al. 2001), we adopt $z = 5.74$ in this paper for quasar spectrum in Vanden Berk et al. (2001).

Table 2. Journal of imaging observations.

Band	Obs. date (UT)	Total integ. time (s)	$m_{\text{lim}}(\text{AB})^*$	$\text{FWHM}_{\text{star}}^{\dagger} (")$
B	2002 February 17	1680	27.1	1.2
R_C	2002 February 15, 16	4800	26.8	1.4
I_C	2002 February 15, 16	3360	26.2	1.2
NB816	2002 February 15 — 17	36000	26.6	0.9
z'	2002 February 15, 16	5160	25.4	1.2

* The limiting magnitude (3σ) with a $2''$ aperture.

[†] The full width at half maximum of stellar objects in the final image.

Table 3. Photometry of a lens galaxy.

Object	B	R_C	I_C	NB816	z'
Lens galaxy	25.1 ± 0.06	24.5 ± 0.04	24.3 ± 0.06	24.2 ± 0.04	23.9 ± 0.09